The Accretion Column
(A Literature Review)

Jörn Wilms

Dr. Karl Remeis-Observatory & ECAP

Friedrich-Alexander-Universität
Erlangen-Nürnberg

ERLANGEN CENTRE
FOR ASTROPARTICLE
PHYSICS

ERLANGEN CENTRE FOR ASTROPARTICLE PHYSICS

Structure

Structure of this talk:

- Accretion in magnetized systems
- Properties of the accretion column
  - rough estimates
  - continuum generation
  - pencil beam vs. fan beam
- CRSF formation: pre 2000

None of the work presented is work by myself

$\Longrightarrow$ "journal club"-type literature review...

And all misunderstandings are mine...

Roche Lobe Overflow

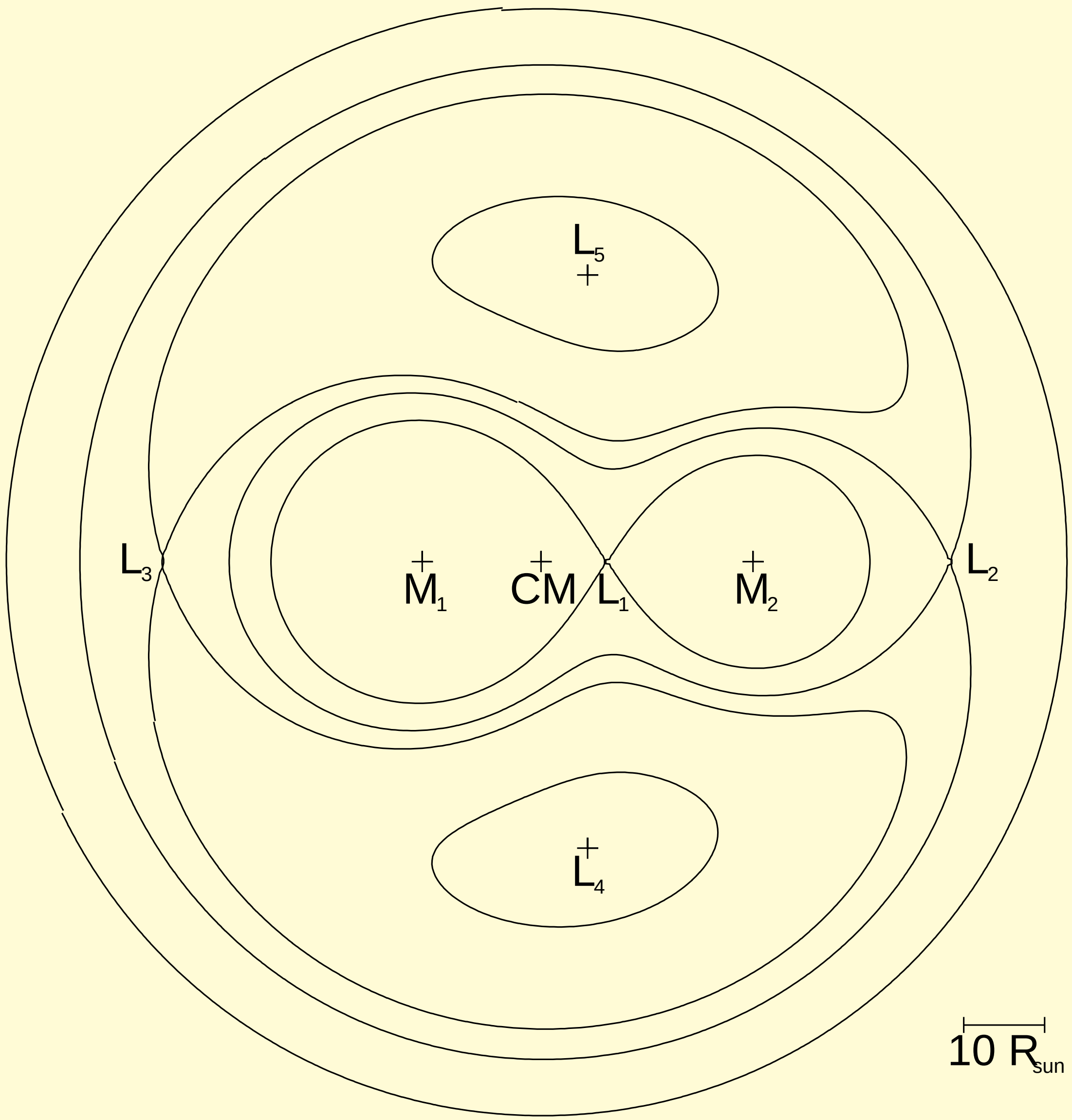

Roche potential:

$$\phi(\boldsymbol{r}) = -\frac{GM_1}{|\boldsymbol{r}-\boldsymbol{r}_1|} - \frac{GM_2}{|\boldsymbol{r}-\boldsymbol{r}_2|} - \frac{1}{2}(\boldsymbol{\omega}\times\boldsymbol{r})^2$$

Stellar evolution: donor star eventually fills Roche lobe

$\Longrightarrow$ Roche Lobe Overflow

$\Longrightarrow$ accretion

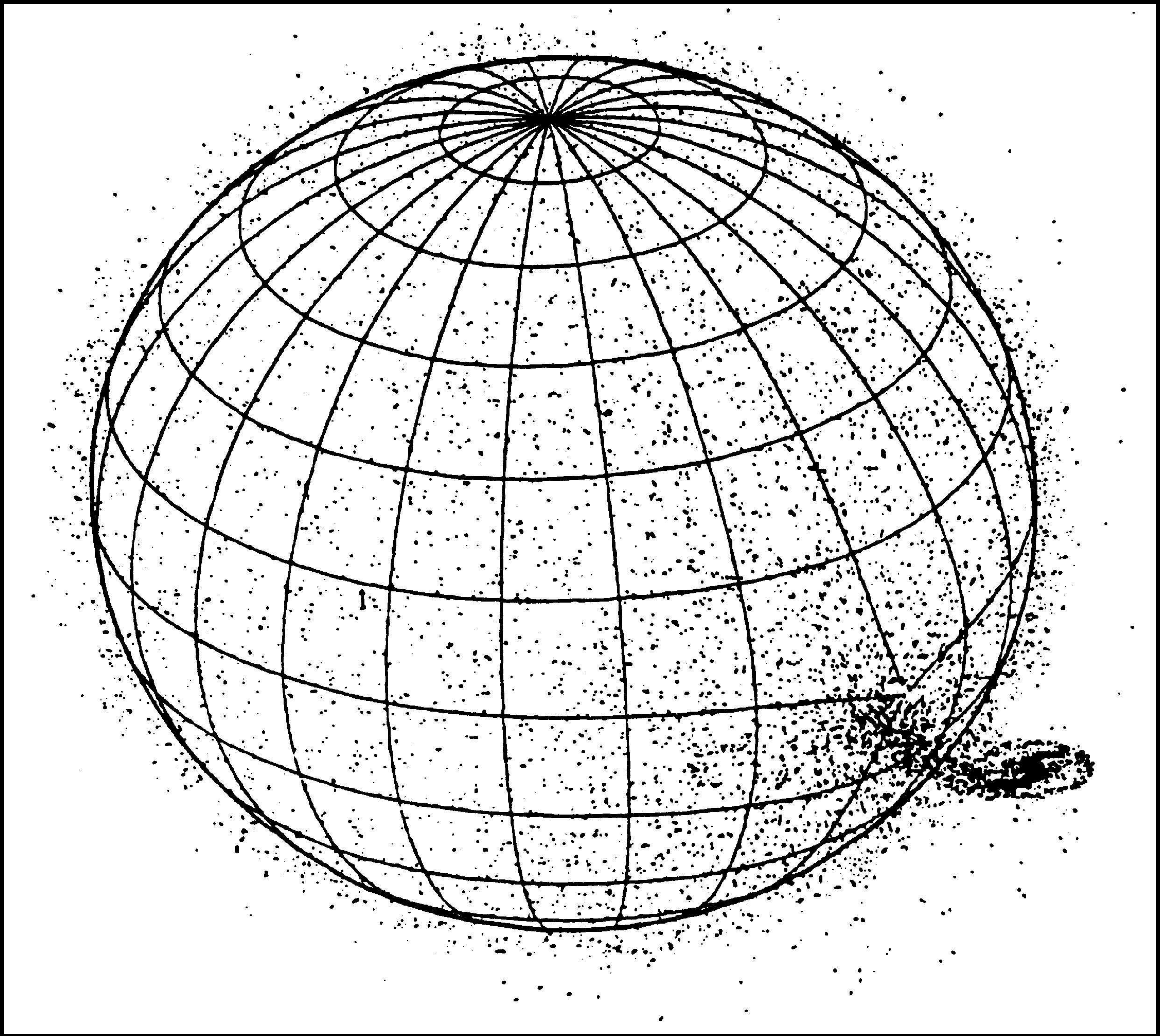

(Dennerl, Dissertation MPE)

Roche Lobe Overflow/focused stellar wind: Matter streams over Lagrange point L_1 from donor onto compact object. Preservation of angular momentum: Formation of accretion disk.

Early type stars: strong winds, driven by radiation pressure in absorption lines.

Typical Mass loss rates: $\dot{M} = 10^{-7...-5}\, M_\odot\, \mathrm{yr}^{-1}$.

Velocity profile:

$$\mathrm{v}(r) \approx \mathrm{v}_\infty \, (1 - R_\star/r)^\beta \quad \text{with} \quad \beta \sim 0.5 \ldots 1.0$$

where $\mathrm{v}_\infty \approx 1000\,\mathrm{km\,s^{-1}}$.

A fraction of the wind ($10^{-4} \ldots 10^{-3}$) can accrete onto compact object: Bondi-Hoyle accretion.

ERLANGEN CENTRE FOR ASTROPARTICLE PHYSICS

Stellar Wind Accretion

Order of magnitude estimates (Ostriker & Davidson, 1973):

Mass accretion rate of neutron star:

$$\dot{M}_{\text{acc}} = \xi \cdot \pi r_{\text{acc}}^2 \cdot v_{\text{rel}} \rho$$

where the accretion radius is

$$r_{\text{acc}} \sim \frac{2GM}{v_{\text{rel}}^2}$$

and where ξ: correction factor for radiation pressure:

$$\xi = \left(1 - 10^{-4.8} (1 + X) \left(\frac{L}{L_\odot} \right) \left(\frac{M}{M_\odot} \right)^{-1} \right)^2$$

Therefore

$$L_{\text{X}} < 10^{4.8} L_\odot \cdot \frac{M}{M_\odot} (1 + X)^{-1} \quad \text{and} \quad \dot{M}_{\text{acc}} < 10^{-7.4} M_\odot \,\text{yr}^{-1} \cdot \frac{M}{M_\odot}$$

Stellar Wind Accretion

Relative velocity between wind and neutron star:

$$v_{\text{rel}}^2 = v_{\text{X}}^2 + v_{\text{w}}^2 = \frac{v_{\text{esc}}^2 R_\star}{2r} + \left(1 - \frac{R_\star}{r}\right)^2 v_\infty^4 = \left(1 - \left(1 - \frac{v_{\text{esc}}^2}{2v_\infty^2}\right)\frac{R_\star}{r}\right) v_\infty^2$$

Density of the stellar wind (continuity eq.):

$$\rho = \frac{\dot{M}_{\text{W}}}{4\pi r^2 v_{\text{W}}} = \frac{\dot{M}_{\text{W}}/4\pi v_\infty}{r^2(1 - R_\star/r)^{1/2}}$$

This then gives

$$\dot{M}_{\text{acc}} = \dot{M}_{\text{W}} \frac{4(M/M_\star)^2\epsilon^2}{(x-1)^{1/2}(x-1+\epsilon)^{3/2}} \left(1 - \frac{L_X}{L_{\text{crit}}}\right)^2$$

where $\epsilon = v_{\text{esc}}^2/2v_\infty^2$ and $x = r/R_\star$.

Comparison with observations then gives mass accretion rates $\lesssim 10^{-7}\,M_\odot\,\text{yr}^{-1}$ (typical $\dot{M} \sim 10^{-9\ldots-11}\,\text{M}_\odot\,\text{yr}^{-1}$)

$10^{-9}\,M_\odot\,\text{yr}^{-1} \sim 6 \times 10^{13}\,\text{kg}\,\text{s}^{-1}$, or 1 IJsselmeer/0.01 sec.

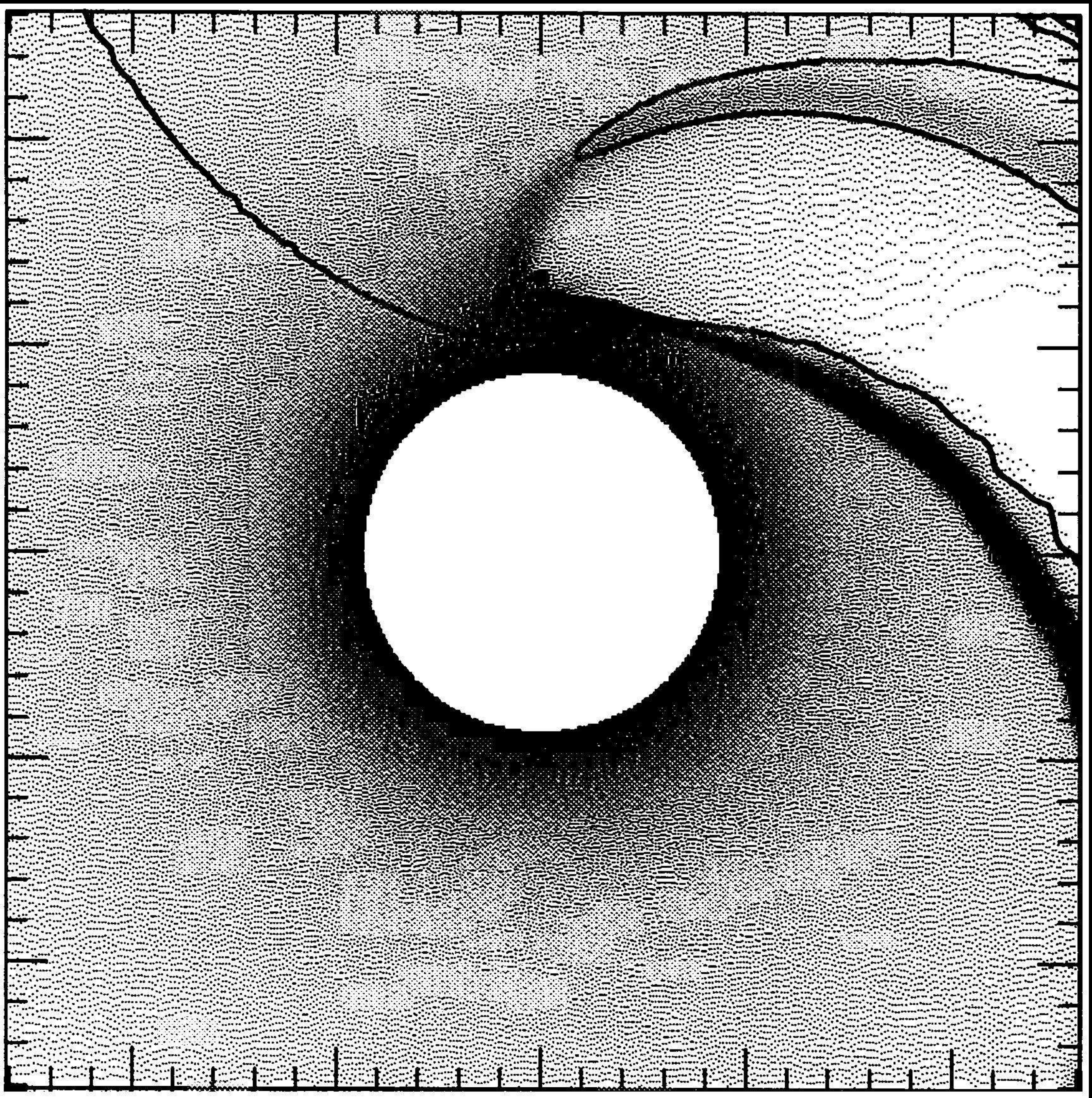

(Blondin (1994), Fig. 4)

Realistic hydrodynamical computations are difficult

(asymmetry of accretion process, ionization of wind, large range of length-scales involved,. . .).

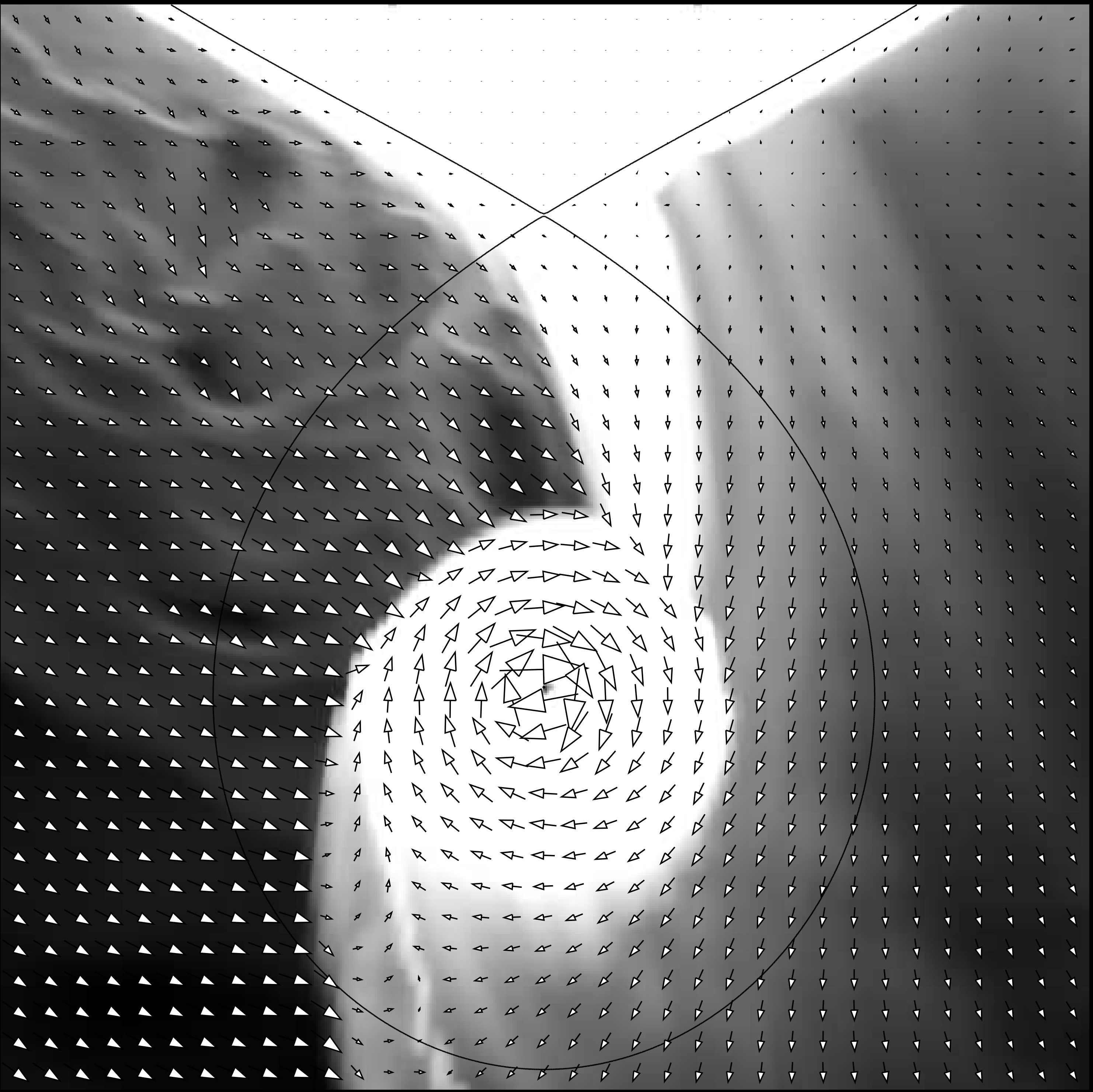

Velocity field from HMXB accretion (simulation for LMC X-4).

(Blondin)

Stellar Wind Accretion

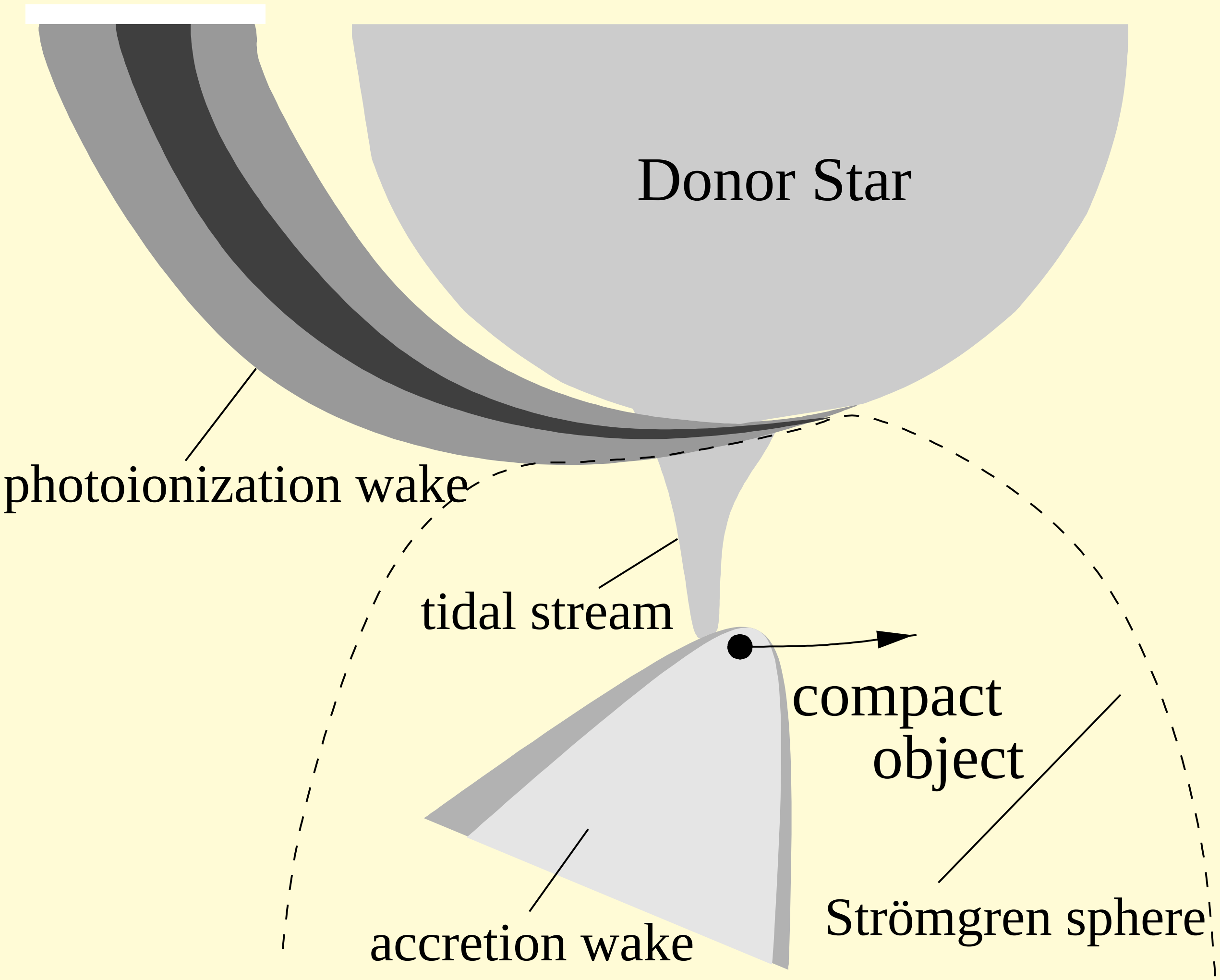

Principal components for wind-accretion:

- Ionized Strömgren region (wind ionized by X-rays from compact object).
- Accretion shock around compact object (since $v_{\mathrm{orb}} > c_{\mathrm{s}}$).
- Ionization wake where material is overdense.

Stellar Wind Accretion

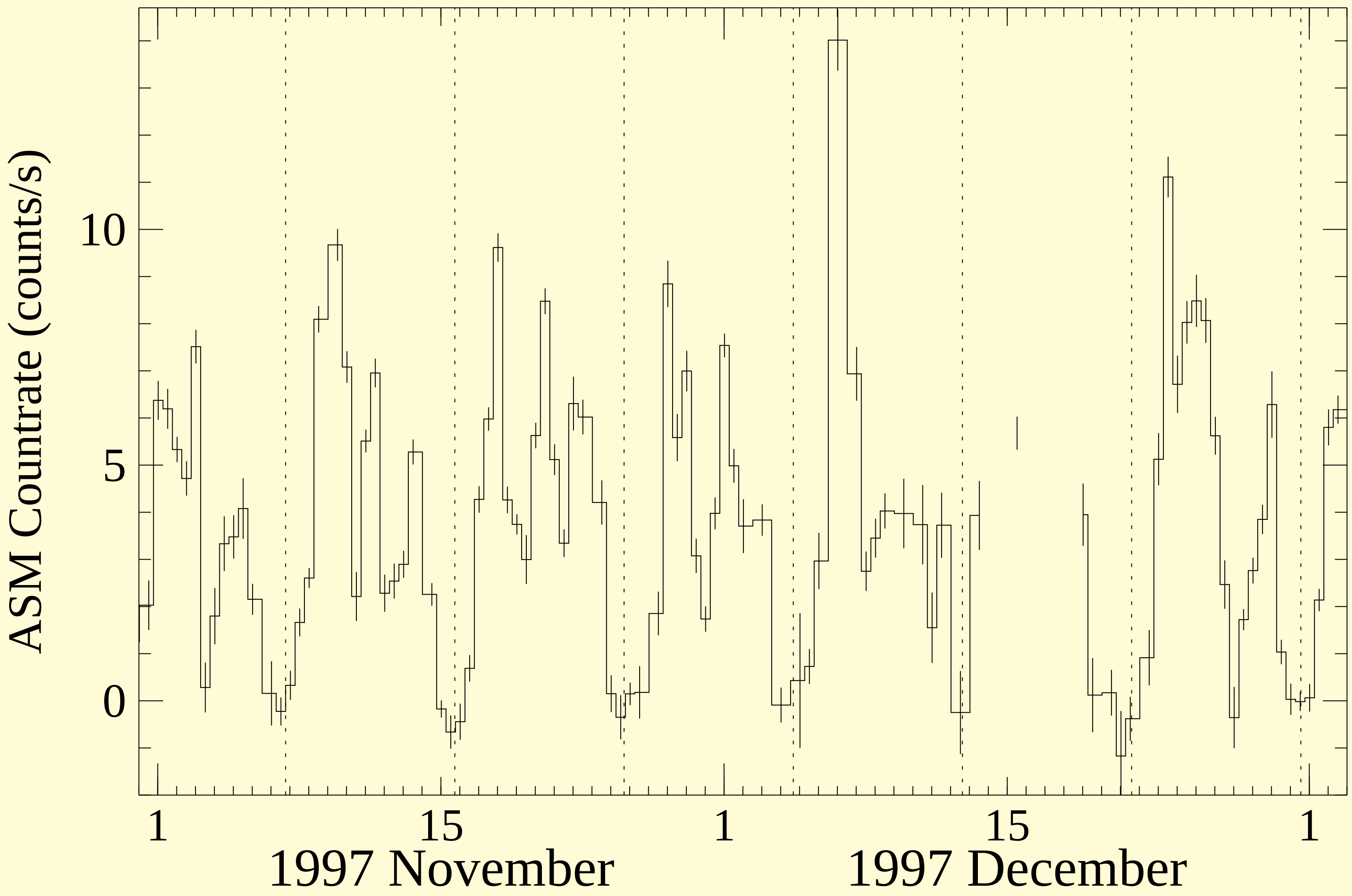

RXTE-ASM 2–10 keV lightcurve of the HMXB Vela X-1

Stellar Wind Accretion

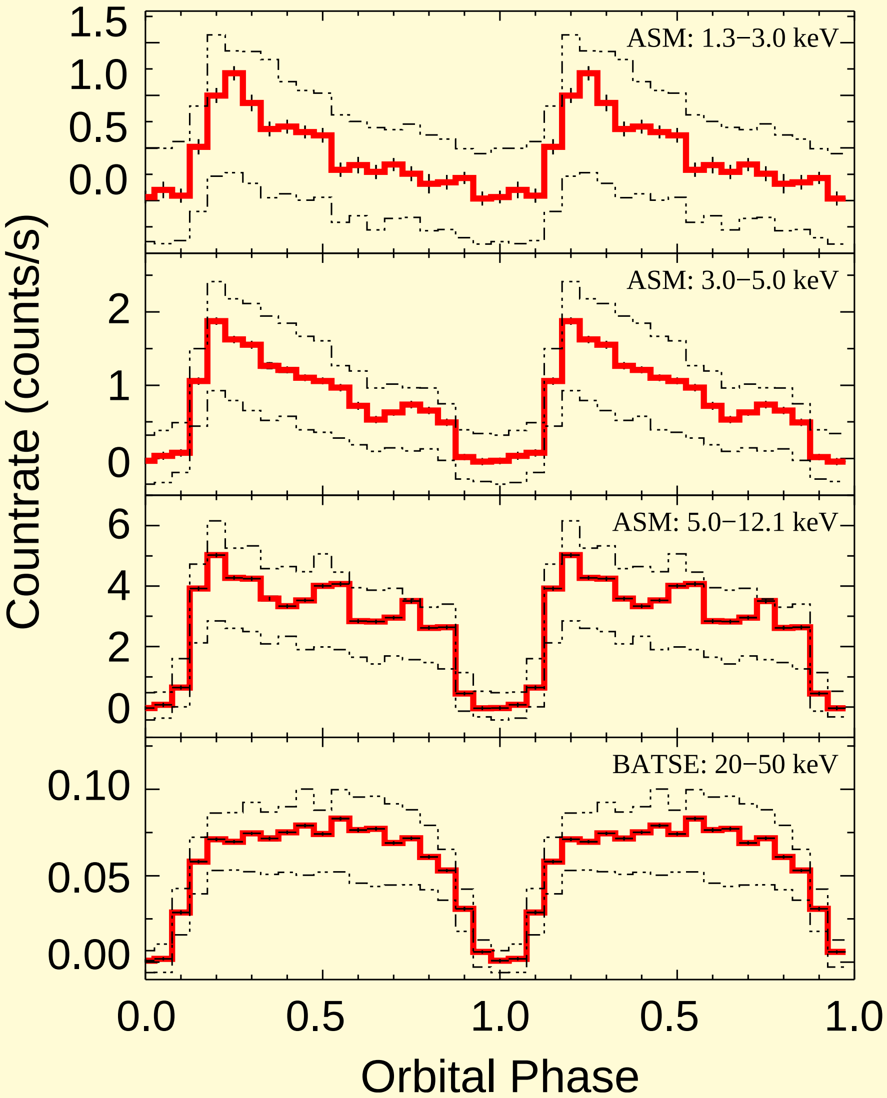

Orbit averaged, energy resolved lightcurves of Vela X-1

See presentations by Fürst/Kreykenbohm and Barragán yesterday.

Magnetospheric Accretion

Neutron stars are expected to have strong B-fields!

Theory

- Flux conservation in SN collapse ($BR^2 =$ const.):

$$\left.\begin{matrix} R \sim 10^{11}\,\text{cm} \\ B \sim 10^{2}\,\text{G} \end{matrix}\right\} \Longrightarrow \left\{\begin{matrix} R \sim 10^{6}\,\text{cm} \\ B \sim 10^{12}\,\text{G} \end{matrix}\right.$$

- post birth generation of dynamo: $\lesssim 10\,\text{G}$ or $\lesssim 10^{12}\,\text{G}$

Observational Estimates

- radio pulsars: magnetic dipole radiation:

$$\frac{\dot{P}}{P} \sim \frac{1}{P^2}\frac{R^4}{M}B^2 \sim 10^{11\ldots13}\,\text{G}$$

- accreting X-ray pulsars: torque theory:

$$-\frac{\dot{P}}{P} \sim P L_{\text{X}}^{6/7} \dot{M} R^{-2/7} B^{2/7} \sim 10^{12}\,\text{G}$$

- *non*-pulsating accreting neutron stars: $\lesssim 10^{9}\,\text{G}$

Measurements: Observations of cyclotron lines yield magnetic fields of several 10^{12} G.

Magnetospheric Accretion

Accretion models has to take into account that central neutron star has $\sim 10^{12}$ G B-field.

Far-field:

$$B(r) = \left(\frac{R}{r}\right)^3 B_\mathrm{p} \quad \text{hence} \quad P_\mathrm{mag} = \frac{B^2}{8\pi} = \left(\frac{R}{r}\right)^6 B_\mathrm{p}^2$$

On the other hand, the accreting material has a ram-pressure

$$P_\mathrm{ram} = \rho v^2 \quad \text{or} \quad P_\mathrm{ram} = \frac{\dot{M}}{4\pi r^2}\left(\frac{2GM}{r}\right)^{1/2}$$

assuming free fall ($v = (2GM/r)^{1/2}$) and spherical symmetry ($\dot{M} = 4\pi r^2 \rho v$).

For $P_\mathrm{mag} > P_\mathrm{ram}$, B-field dominates $\Longrightarrow$ plasma couples to B-field lines at the Alfvén radius

$$r_\mathrm{mag} = \left(\frac{8\pi^2}{G}\right)^{1/7} \left(\frac{R^{12}B_\mathrm{p}^4}{M\dot{M}^2}\right)^{1/7}$$

$$= 1800\,\mathrm{km} \left(\frac{R}{10\,\mathrm{km}}\right)^{12/7} \left(\frac{B}{10^{12}\,\mathrm{G}}\right)^{4/7} \left(\frac{M}{1.4\,M_\odot}\right)^{-1/7} \left(\frac{\dot{M}}{10^{-7}\,M_\odot\,\mathrm{yr}^{-1}}\right)^{-2/7}$$

For typical NS parameters, the accretion close to the NS is dominated by the B-field.

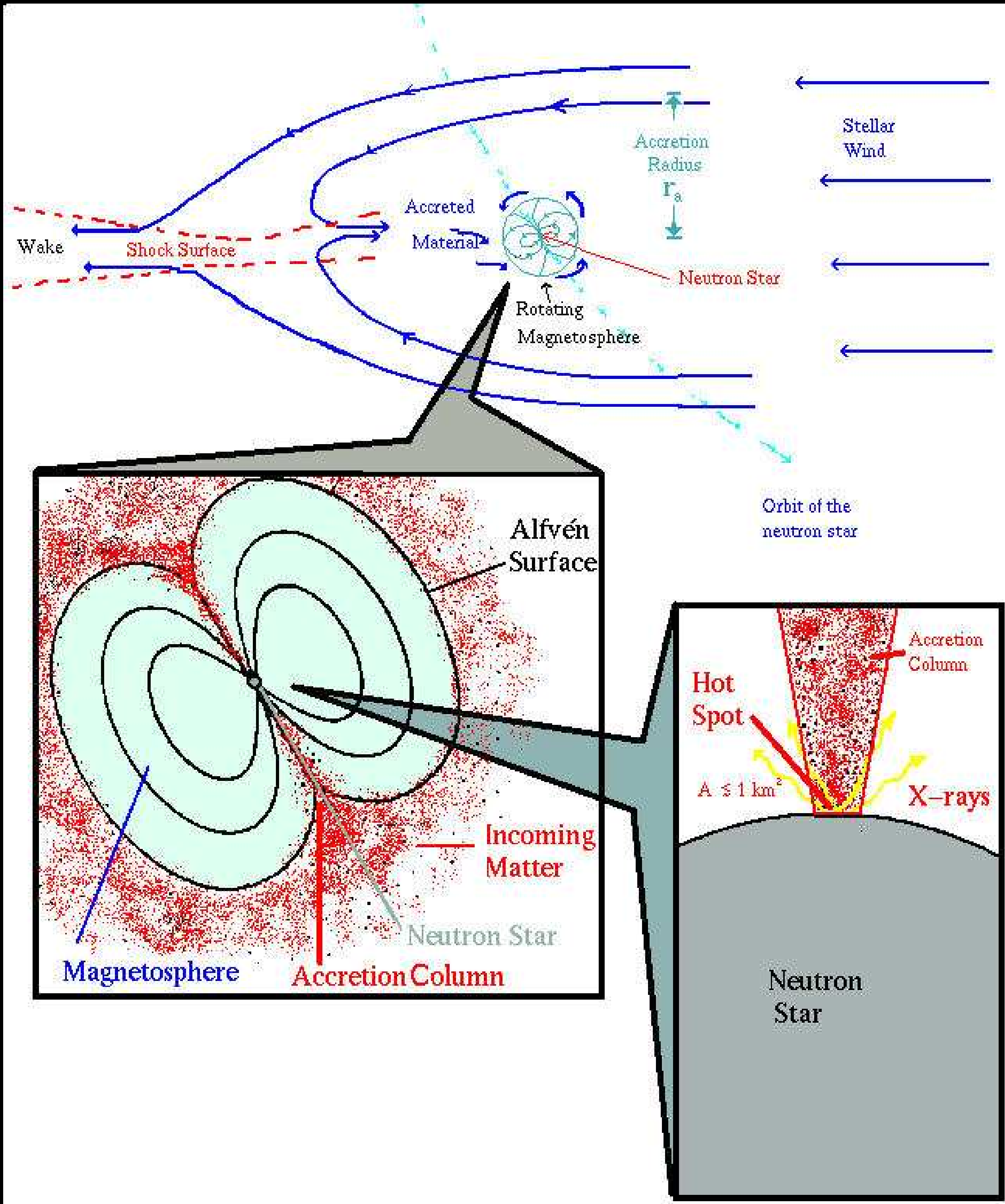

courtesy I. Negueruela, based on Davidson & Ostriker (1973)

The Neutron Star Poles

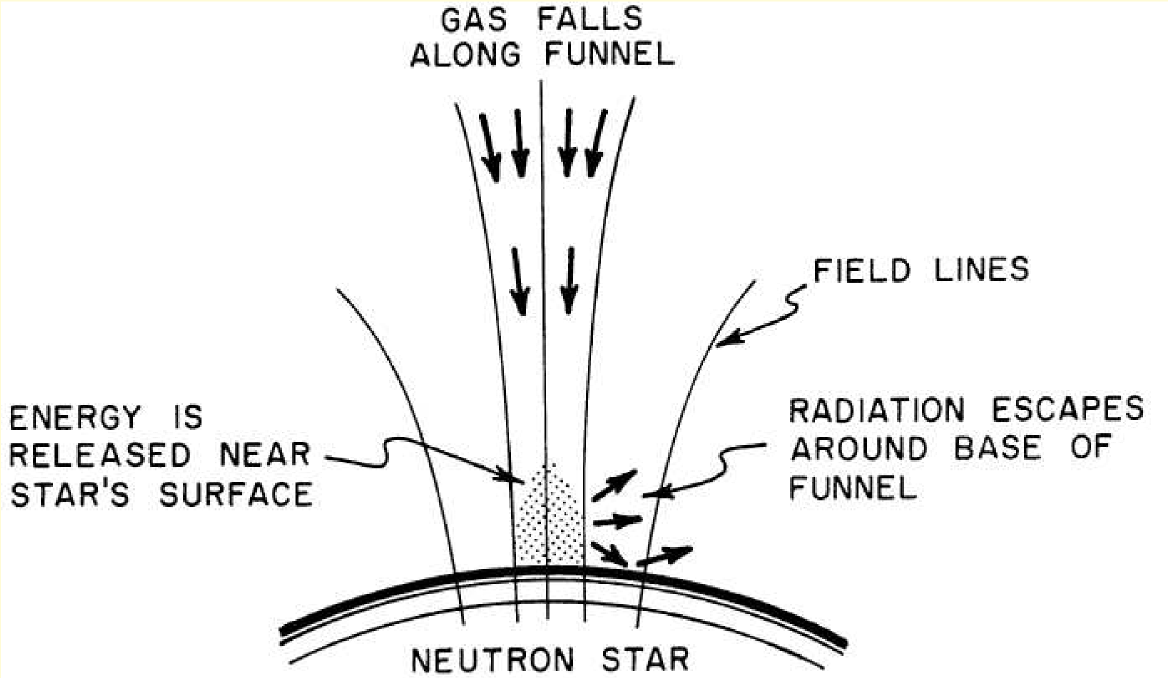

(Ostriker & Davidson, 1973, Fig. 4)

Within R_{mag}, low density material

$\Longrightarrow$ approximate free fall along B-field lines.

Speed at magnetic pole:

$$v = \sqrt{\frac{2GM}{R}} \sim 0.65\,c$$

($\sim$140 MeV nucleon^{-1})

The radius of accretion spot is (for a dipolar B-field):

$$r_0 = R^{3/2} R_{\text{mag}}^{-1/2} \sim 0.8\,\text{km}$$

see also Pringle & Rees (1972), Gnedin & Sunyaev (1973), and Inoue (1975).

The Neutron Star Poles

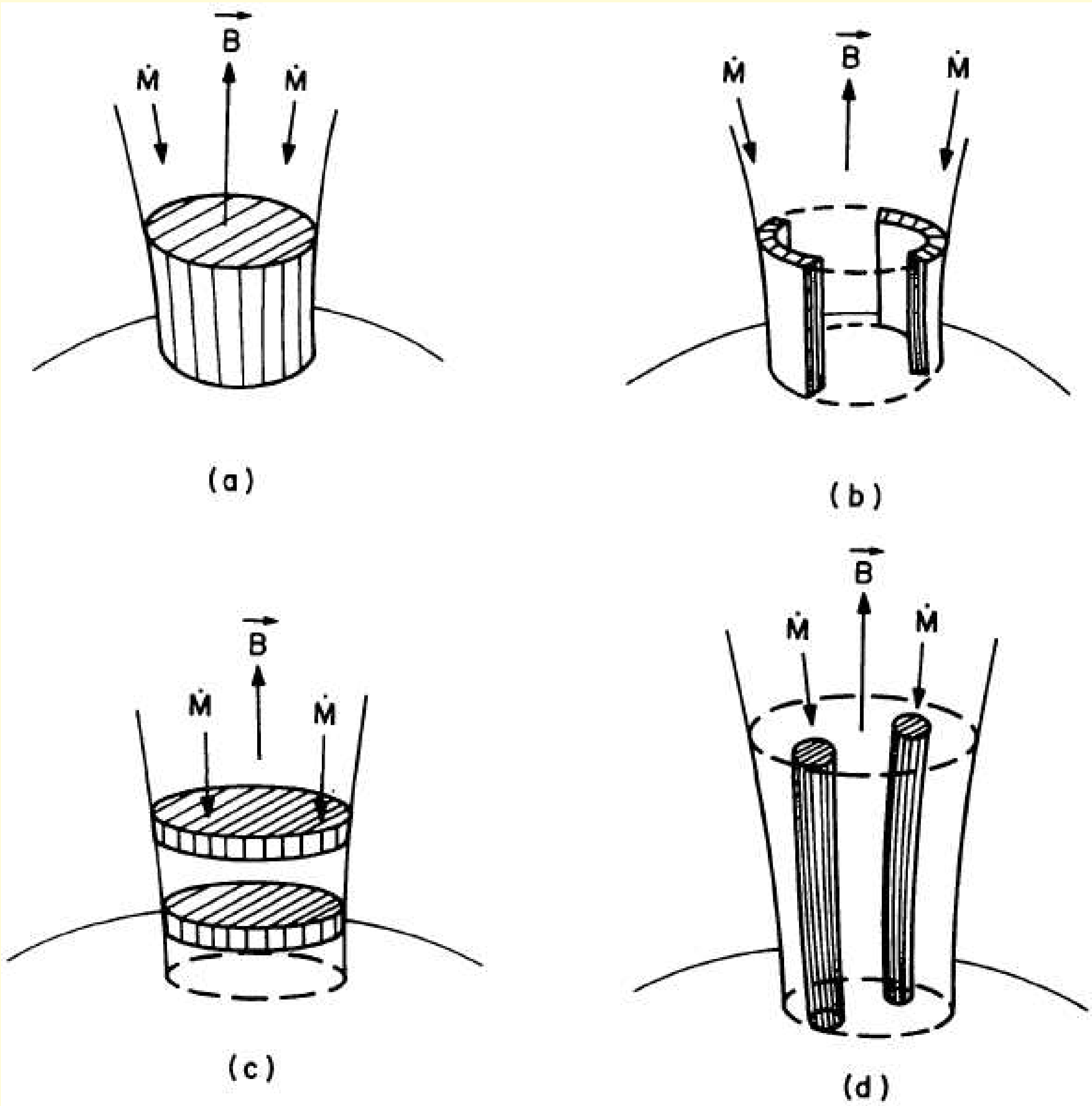

Note: Whether accretion column is filled, a hollow funnel, or "spaghetti like" depends on the details of the coupling of the accretion disk to the B-field, which is not really understood.

(Mészáros, 1984, Fig. 11)

Basic Theory

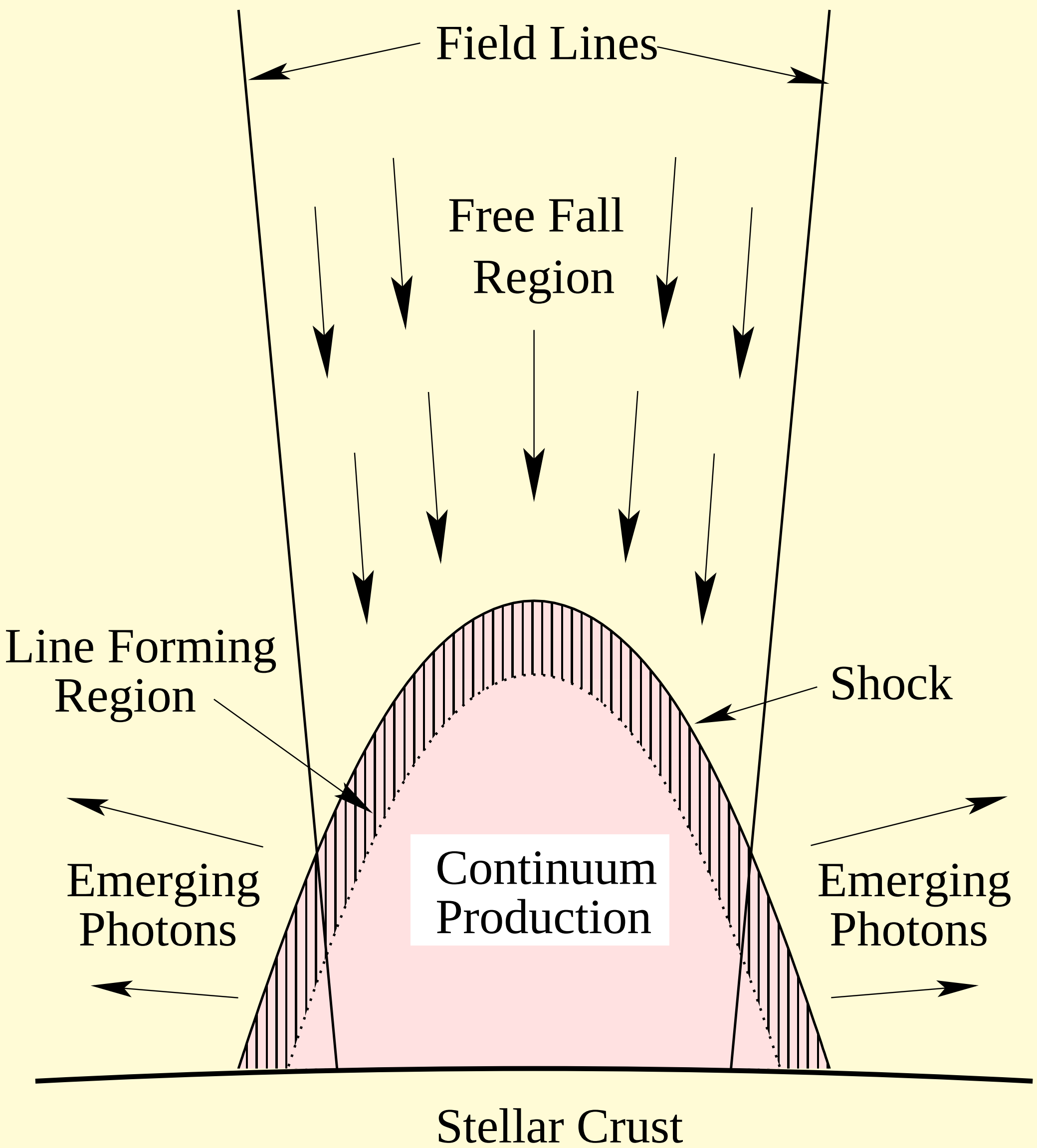

Basic idea of continuum formation:

1. shock $\Longrightarrow$ low energy photons (bremsstrahlung)
2. Compton upscattering in accretion mound/column
3. Photons emerge once $\tau < 1$

Most important process modifying continuum: resonant Compton scattering

(Heindl et al., 2004)

Landau Levels

Strong field at NS poles: Quantization of electron energies $\perp B$-field lines (Landau levels):

$$E_n = m_\mathrm{e}c^2 \frac{\sqrt{1 + 2n(B/B_\mathrm{crit})\sin^2\theta} - 1}{\sin^2\theta}$$

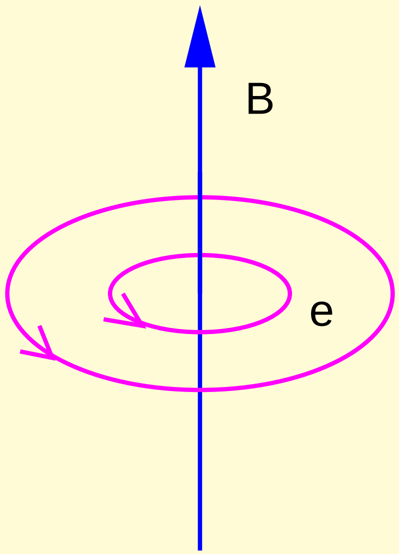

$p_\parallel$: momentum of electron $\parallel B$-field, n: major quantum number, B_crit is

$$B_\mathrm{crit} = \frac{m_\mathrm{e}^2 c^3}{\mathrm{e}\hbar} \sim 4.4 \times 10^{13}\,\mathrm{G}$$

For $B \ll B_\mathrm{crit}$, distance between Landau levels:

$$E_\mathrm{cyc} = \frac{\hbar e}{m_\mathrm{e}c} B = 11.6\,\mathrm{keV} \left(\frac{B}{10^{12}\,\mathrm{G}}\right)$$

($12 - B_{12}$-rule)

$\Longrightarrow$ Cyclotron Resonance Scattering Features ("Cyclotron lines") at

$$E_n = nE_\mathrm{cyc} = (1+z)E_{n,\mathrm{obs}}$$

($1 + z \sim 1.25 \ldots 1.4$; grav. redshift!)

Landau Levels

Transition rules from state $(n, s, p) \leftrightarrow (n', s', p')$ ($s = (\sigma_z + 1)/2$) (e.g., Harding & Lai 2006):

$$E_n - E_{n'} = \pm\epsilon \quad \text{and} \quad p' = p \mp \epsilon\cos\theta$$

with

$$\epsilon = \pm\frac{1}{\sin^2\theta}(E_n - p\cos\theta) - \left((E_n - p\cos\theta)^2 - 2B'(n-n')\sin^2\theta\right)^{1/2}$$

where $p = cp_z$, energy units are in $m_\mathrm{e}c^2$ and where $B' = B/B_\mathrm{crit}$.

The absorption cross section is (Harding & Daugherty, 1991)

$$\sigma^N_\mathrm{abs}(\|, \perp) = \frac{2\alpha\pi^2\bar{\lambda}^2}{E_N}\delta(\epsilon_N - \epsilon)\frac{e^{-Z}Z^{N-1}}{(N-1)!}\left((\cos^2\theta, 1) + \frac{Z}{N}(\sin^2\theta, 0)\right)$$

with

$$Z = \frac{\epsilon^2\sin^2\theta}{2B'}, \quad \bar{\lambda} = \frac{\hbar}{m_\mathrm{e}c}, \quad \alpha = 1/137$$

Landau Levels

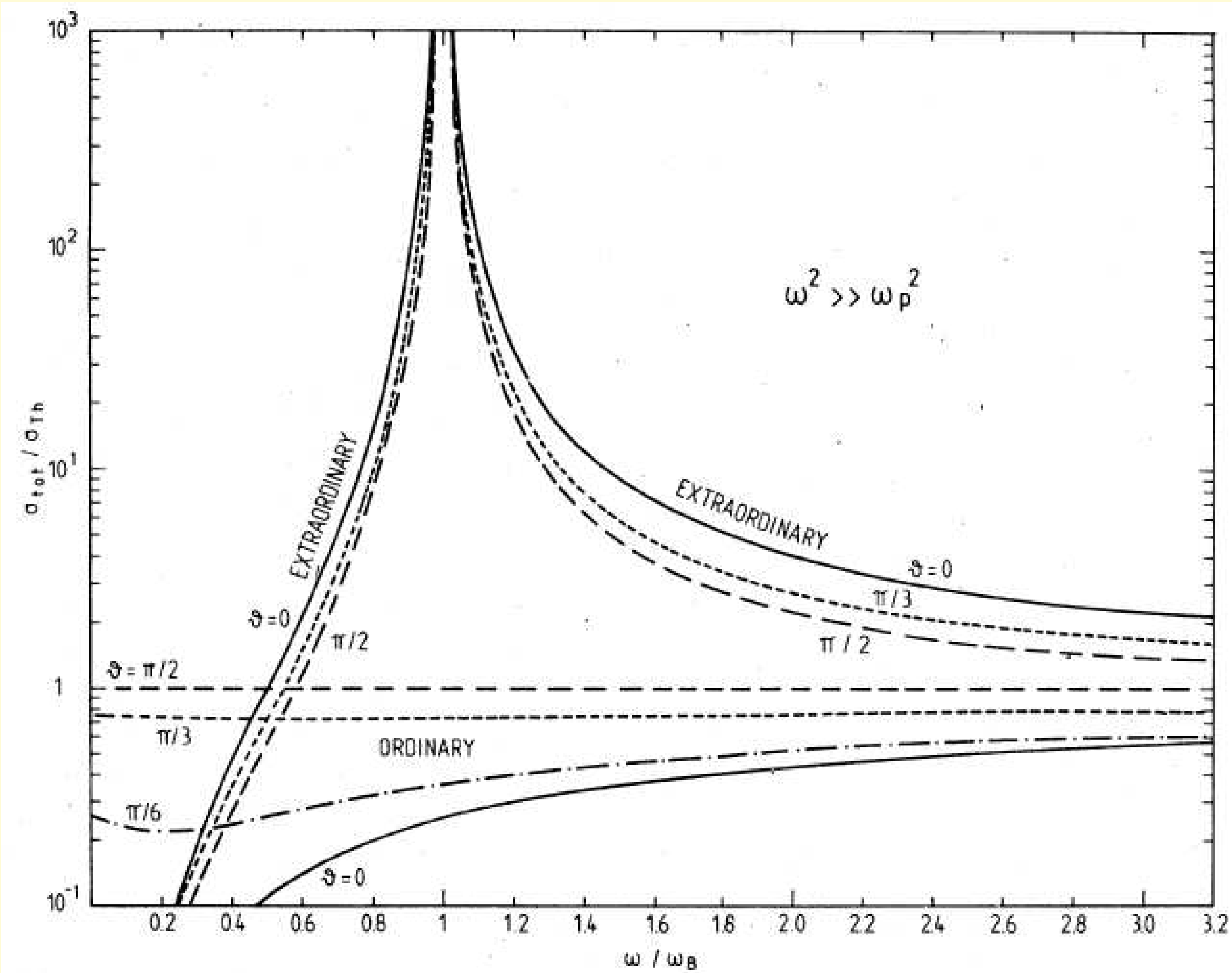

Radiation in accretion column interacts with resonant electrons $\Longrightarrow$ strong freq. dependence of the scattering cross section

Ventura (1979, Fig. 2), see Gonthier et al. (2000) for good approximations to the cross sections, and, e.g., Canuto (1970) and Canuto, Lodenquai & Ruderman (1971) for early work.

Landau Levels

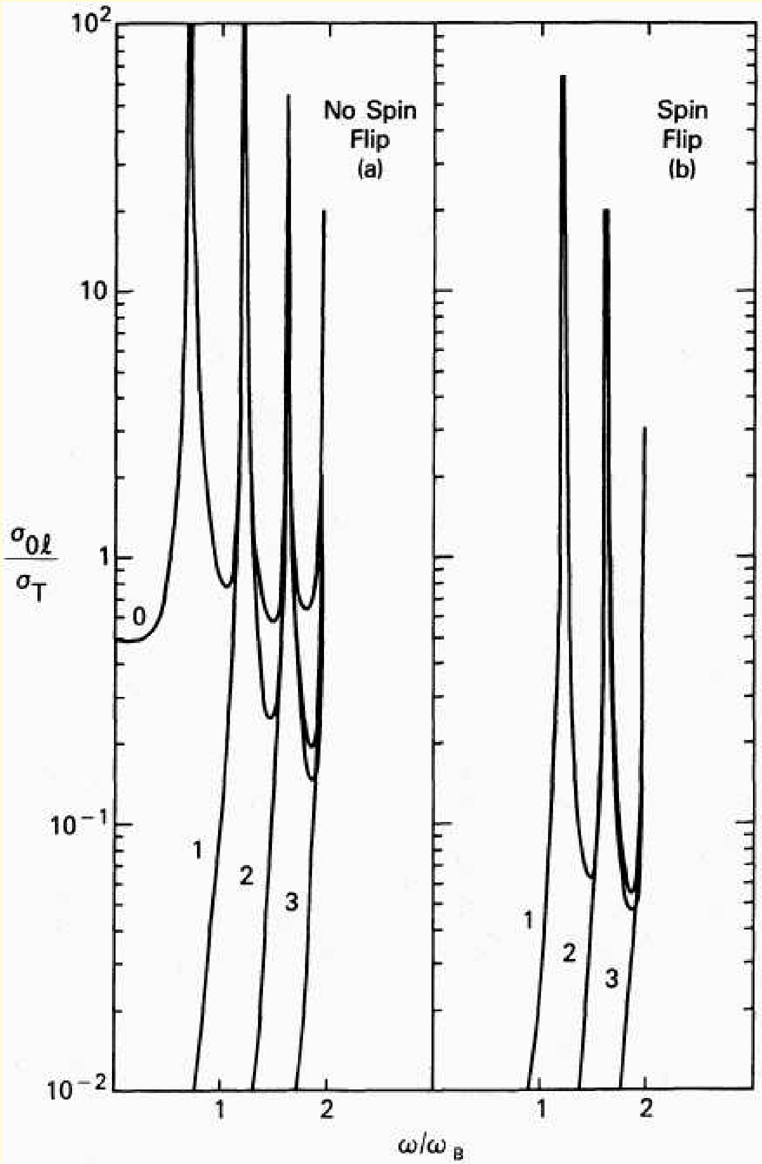

Daugherty & Harding (1986); Harding & Daugherty (1991): Refined cross sections for resonant Compton scattering including transitions to arbitrary Landau levels, photon splitting,. . .

(Daugherty & Harding, 1986, Fig. 2, incident photon angle is 90°)

Accretion Column

Interaction of continuum radiation with electrons (Arons, Klein & Lea, 1987):

Ordinary mode: E-field of photons in plane spanned by B-field and propagation direction. Continuum process only!

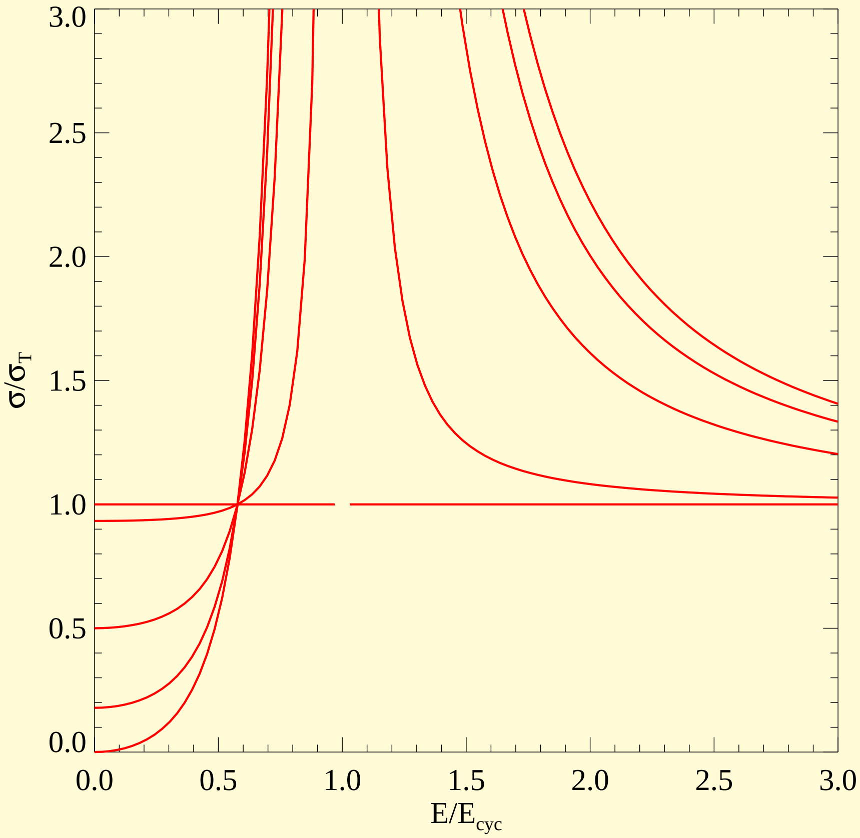

Cross section:

$$\sigma_{\mathrm{ord}}(\varphi) \sim \sigma_{\mathrm{T}} \left(\sin^2 \varphi + k(\epsilon) \cos^2 \varphi\right)$$

where

$$k(\epsilon) = \begin{cases} 1 & \text{for } E \gg E_{\mathrm{cyc}} \\ (E/E_{\mathrm{cyc}})^2 & \text{for } E \ll E_{\mathrm{cyc}} \end{cases}$$

and where $\phi = \angle(\boldsymbol{B}, \text{dir. propagation})$.

(using notation of Becker & Wolff, 2007, see Blandford & Scharlemann 1976 for exact nonrelativistic cross sections)

Accretion Column

Extraordinary mode: E-field of photons perpendicular to plane spanned by B-field and direction of propagation.

Continuum *and* resonant scattering possible.

Cross section:

$$\sigma_{\text{ext}}(\varphi) = \sigma_{\text{T}} k(\epsilon) + \sigma_\ell \phi_\ell(E, E_{\text{cyc}}, \varphi)$$

where

- σ_ℓ: resonant cross section,

$$\sigma_\ell \sim 1.9 \times 10^4 \frac{\sigma_{\text{T}}}{B_{12}}$$

- $\phi_\ell(E, E_{\text{cyc}}, \varphi)$: line profile

  ($\sim$ Gaussian if taking thermal broadening into account)

Accretion Column

Approximate cross sections outside of resonance:

Mode averaged cross section $\parallel \boldsymbol{B}$ ($\varphi = 0^\circ$):

$$\sigma_{\parallel} = \frac{1}{2}\left(\sigma_{\text{ord}}(0^\circ) + \sigma_{\text{ext}}(0^\circ)\right) \sim \sigma_{\text{T}} \left(\frac{E}{E_{\text{cyc}}}\right)^2$$

Mode averaged cross section $\perp \boldsymbol{B}$ ($\varphi = 90^\circ$):

$$\sigma_{\perp} = \frac{1}{2}\left(\sigma_{\text{ord}}(90^\circ) + \sigma_{\text{ext}}(90^\circ)\right) = \sigma_{\text{T}} + \sigma_{\text{T}} \left(\frac{E}{E_{\text{cyc}}}\right)^2 \sim \sigma_{\text{T}}$$

Plasma is much more transparent parallel to the B-field than perpendicular to the B-field!

For order of magnitude estimates, use mean energy of radiation field, $\langle E\rangle$, instead of E in above equations.

Accretion Column

Basko & Sunyaev (1976): Radiation pressure becomes important once

$$L_X \sim L_{crit} = 2.72 \times 10^{37}\,\mathrm{erg\,s^{-1}}\,\frac{\sigma_T}{\sqrt{\sigma_\perp \sigma_\parallel}}\left(\frac{M}{M_\odot}\right)\left(\frac{r_0}{R}\right)$$

For $L_X \gtrsim L_{crit}$ flow is super-Eddington and radiation pressure $\gg$ gas pressure.

$\Longrightarrow$ radiation pressure dominated shock

("accreted matter acts as test particles").

implies continuous velocity transition over few Thomson lengths, different from traditional hydrodynamical shocks!

For $L_X \lesssim L_{crit}$: breaking of plasma by hydrodynamical shock, "Coulomb friction", or nuclear collisions (stopping length $\sim$30–60 $\mathrm{g\,cm^{-2}}$).

see, e.g., Basko & Sunyaev (1976), Langer & Rappaport (1982), Braun & Yahel (1984), Karino, Kino & Miller (2008)

What physical process is the most important is still very much debated.

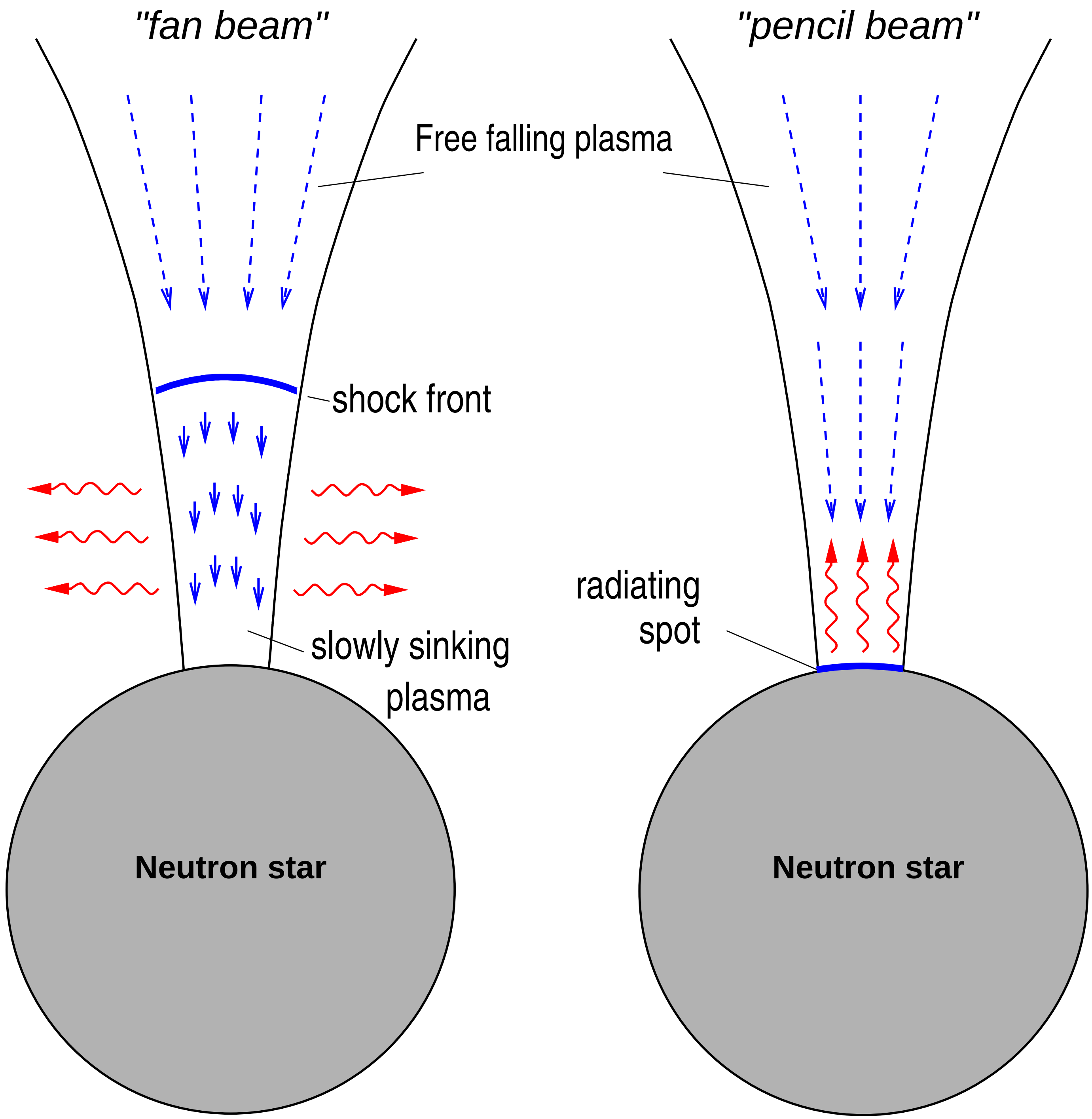

(Kretschmar 1996, Dissertation AIT, Abb. 2.9 [after Harding 1994])

$\Longrightarrow$ “cylinder” and “slab geometries” for emission calculations

Continuum Formation: History

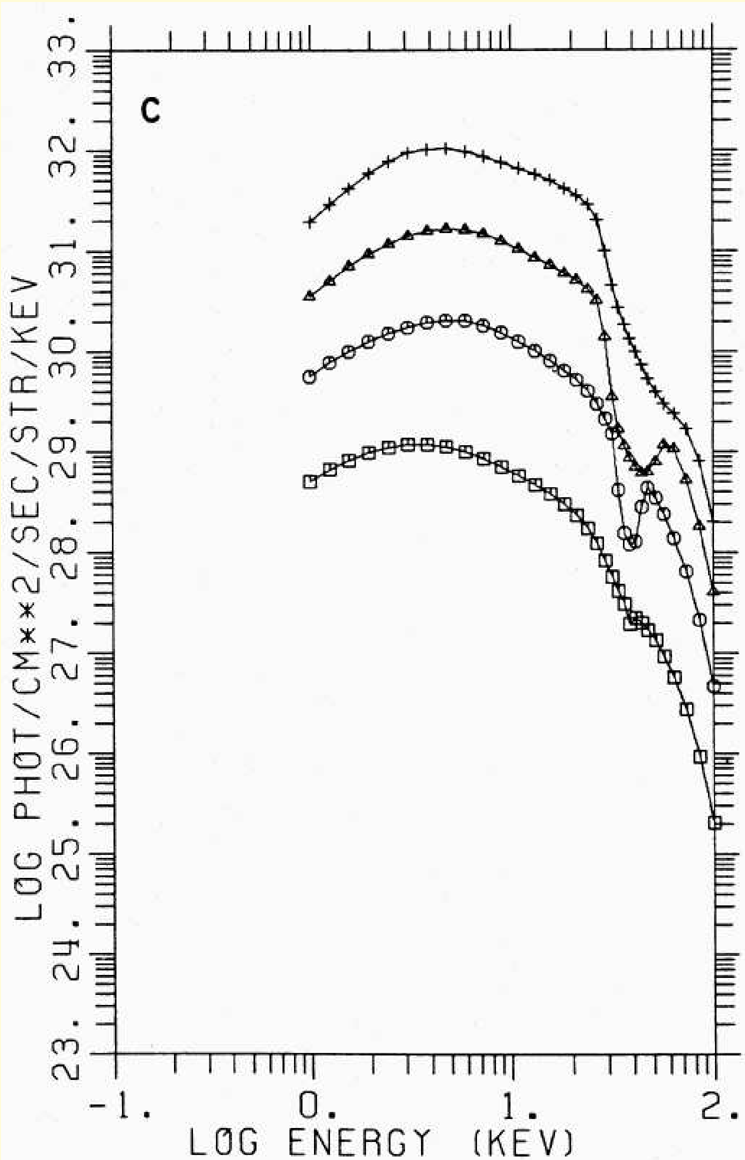

First simple models for accretion column by Nagel (1981a,b), still using two-stream approximation etc.

Mészáros & Nagel (1985a,b): angle dependent calculations based on Feautrier methods.

get continua $\sim$ right (about one order of magnitude)

Spectra emerging from a slab (top to bottom $\theta = 21^\circ$, 48°, 71°, and 86°; Mészáros & Nagel 1985a, Fig. 3c)

Continuum Formation: History

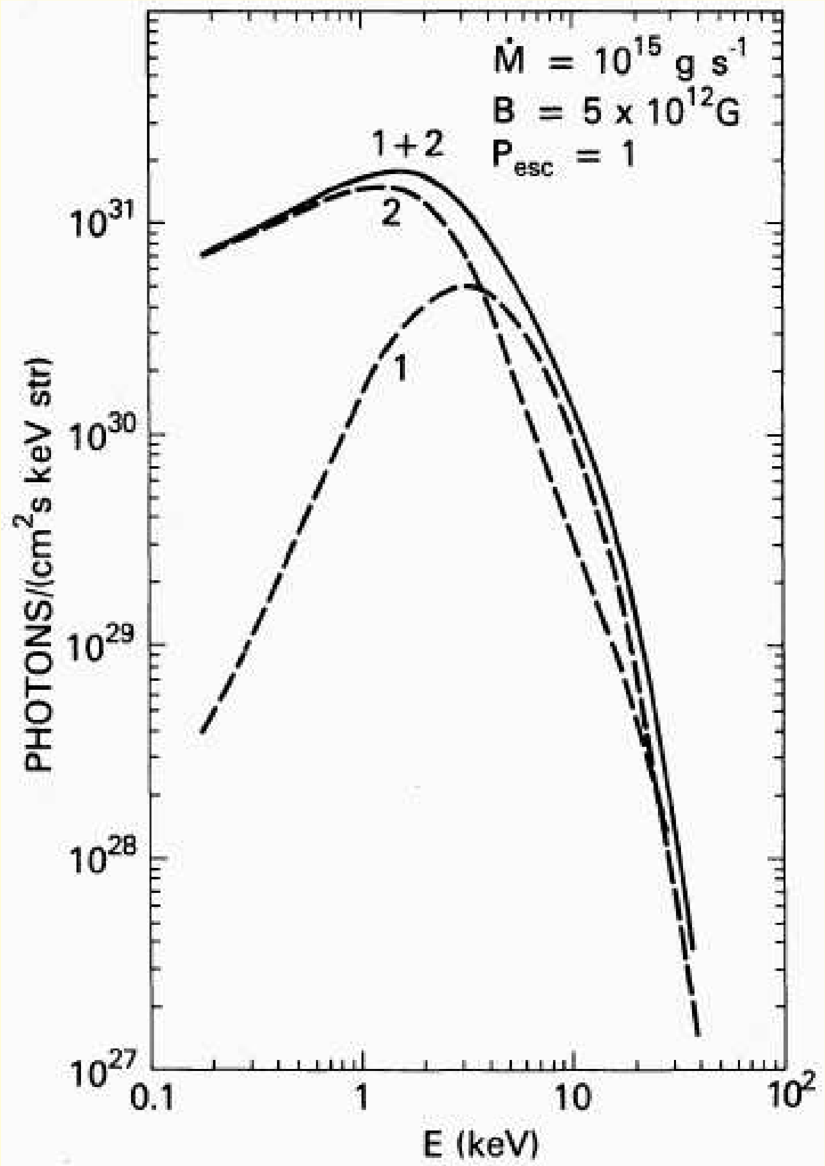

Emission from a column where accretion is stopped by Coulomb interactions

$\Longrightarrow$ reproduction of basic neutron star spectral shape not too bad...

($B = 5 \times 10^{12}$ G, 1: extraordinary mode, 2: ordinary mode Harding et al., 1984)

Continuum Formation: History

Ginga observations of GRB 870303 and GRB 880205: spectral features at 20 keV and 40 keV, interpreted as cyclotron lines $\Longrightarrow$ flurry of activities.

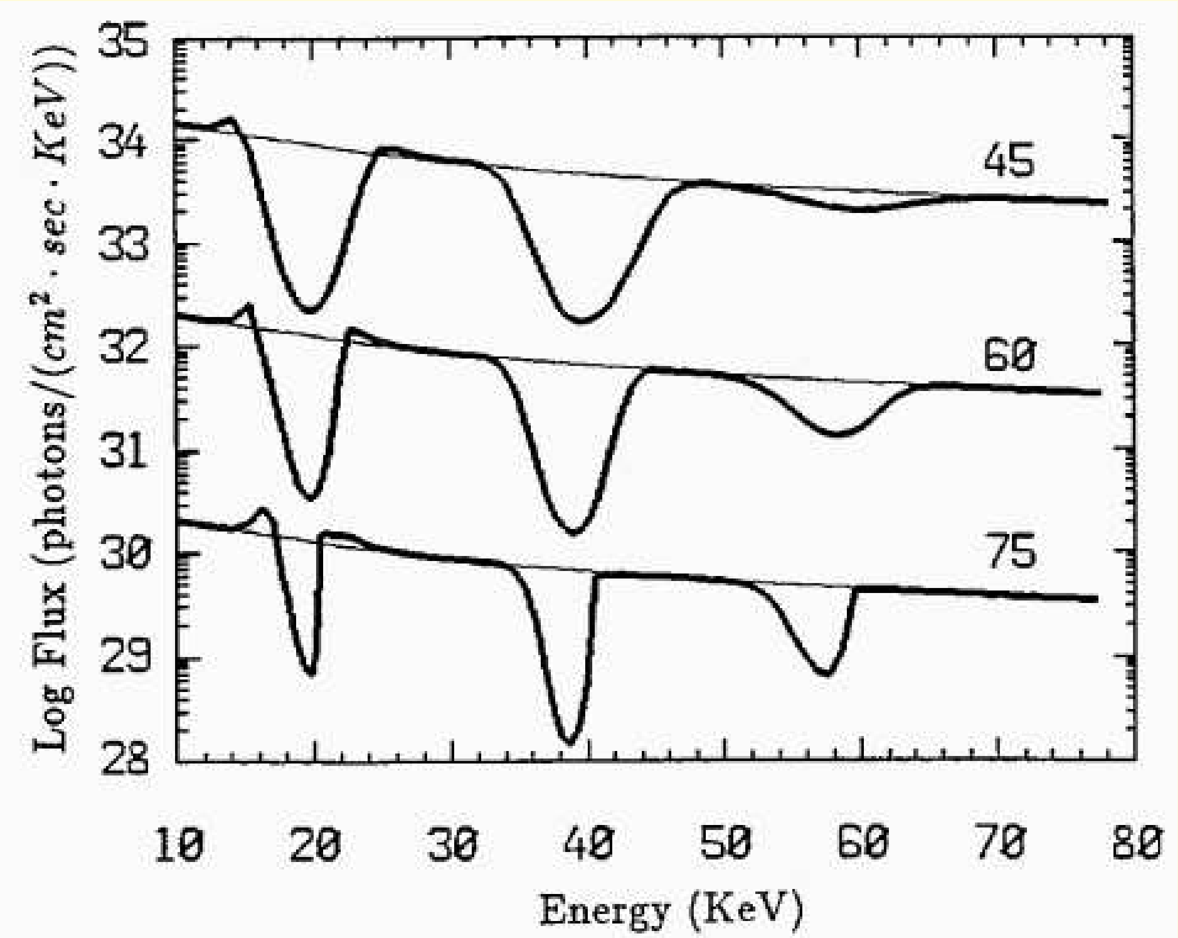

Example: Line shape calculations by Alexander & Mészáros (1989).
$\Longrightarrow$ note the emission wings!

Similar results also by Freeman et al. (1999), Wang et al. (1989) and others.

Continuum Formation: History

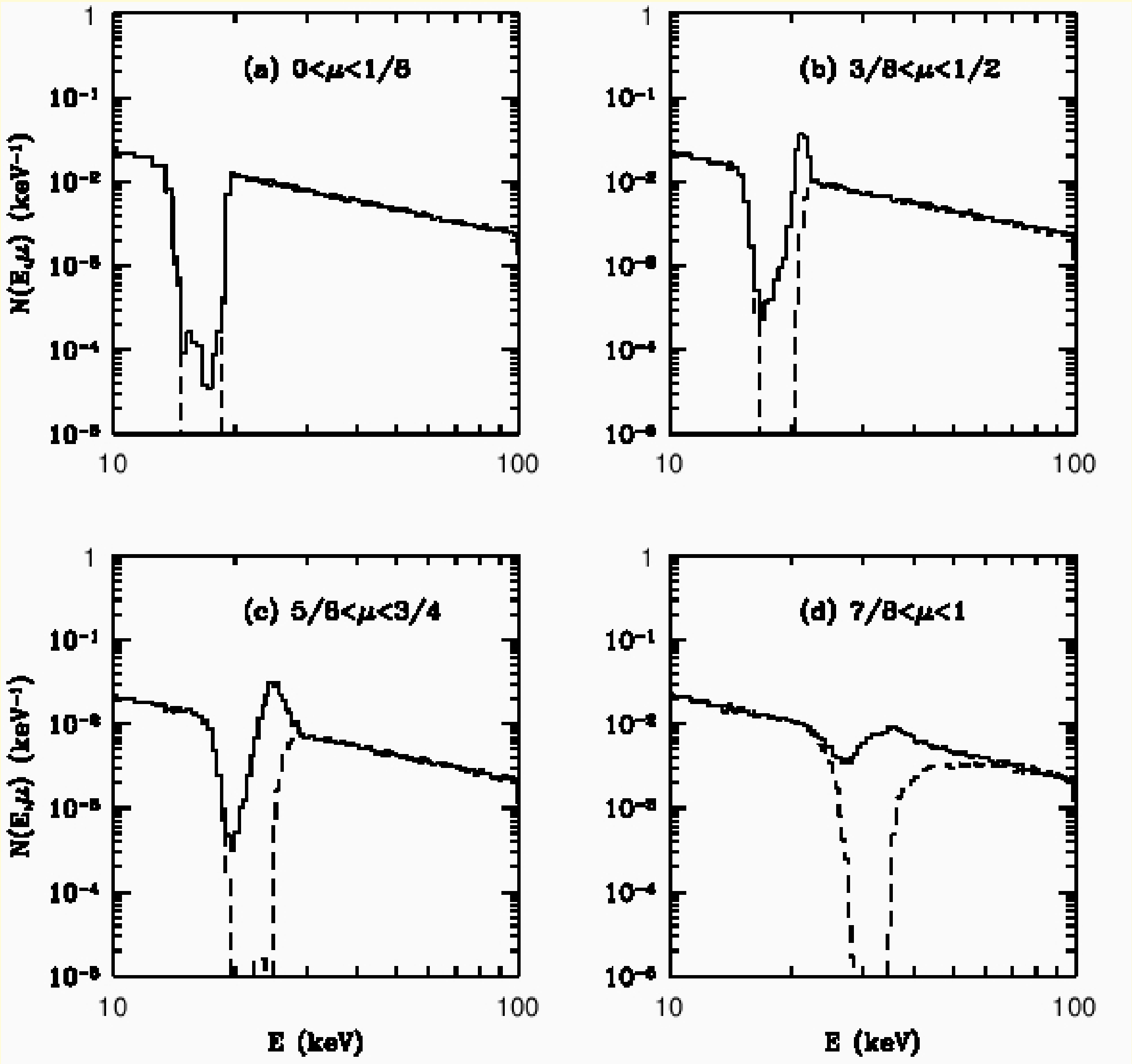

Isenberg, Lamb & Wang (1998a): effects of bulk motion (outflow) on CRSF shape

Continuum Formation: History

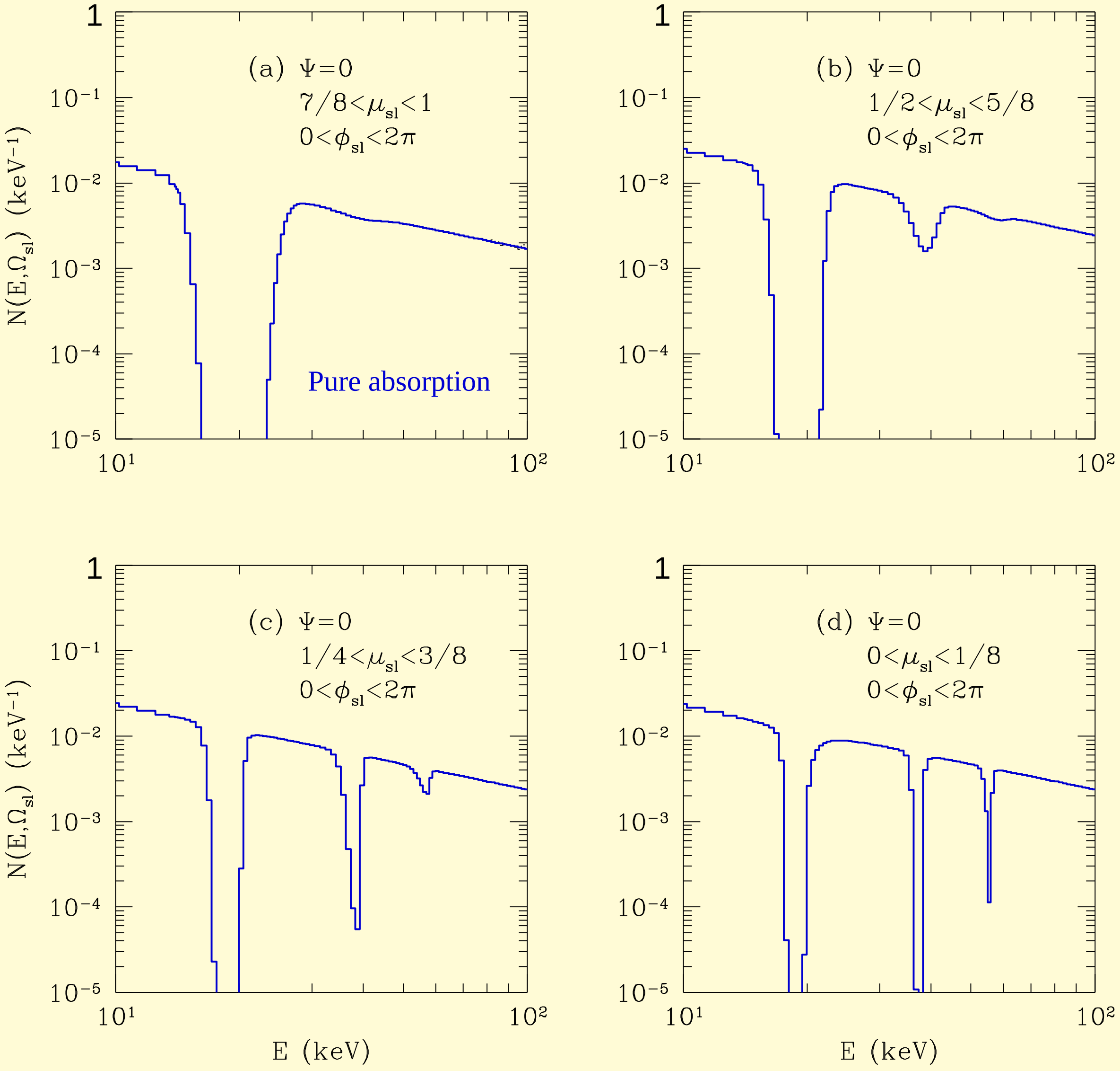

Isenberg, Lamb & Wang (1998b): dependence of the geometry on the CRSF shape

$\Longrightarrow$ see talks by Nishimura and Schönherr for more!

Continuum Formation: History

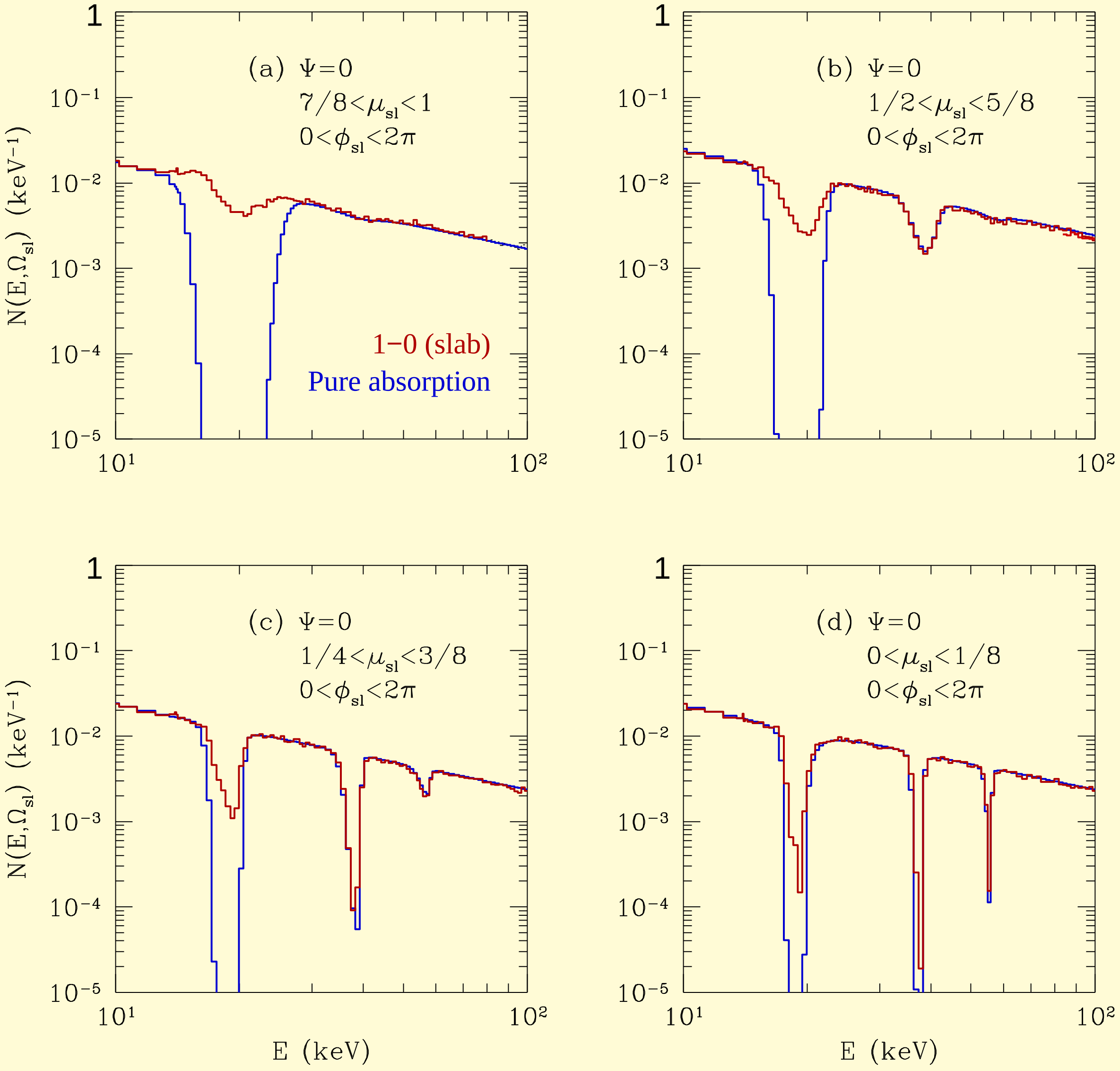

Isenberg, Lamb & Wang (1998b): dependence of the geometry on the CRSF shape

$\Longrightarrow$ see talks by Nishimura and Schönherr for more!

Continuum Formation: History

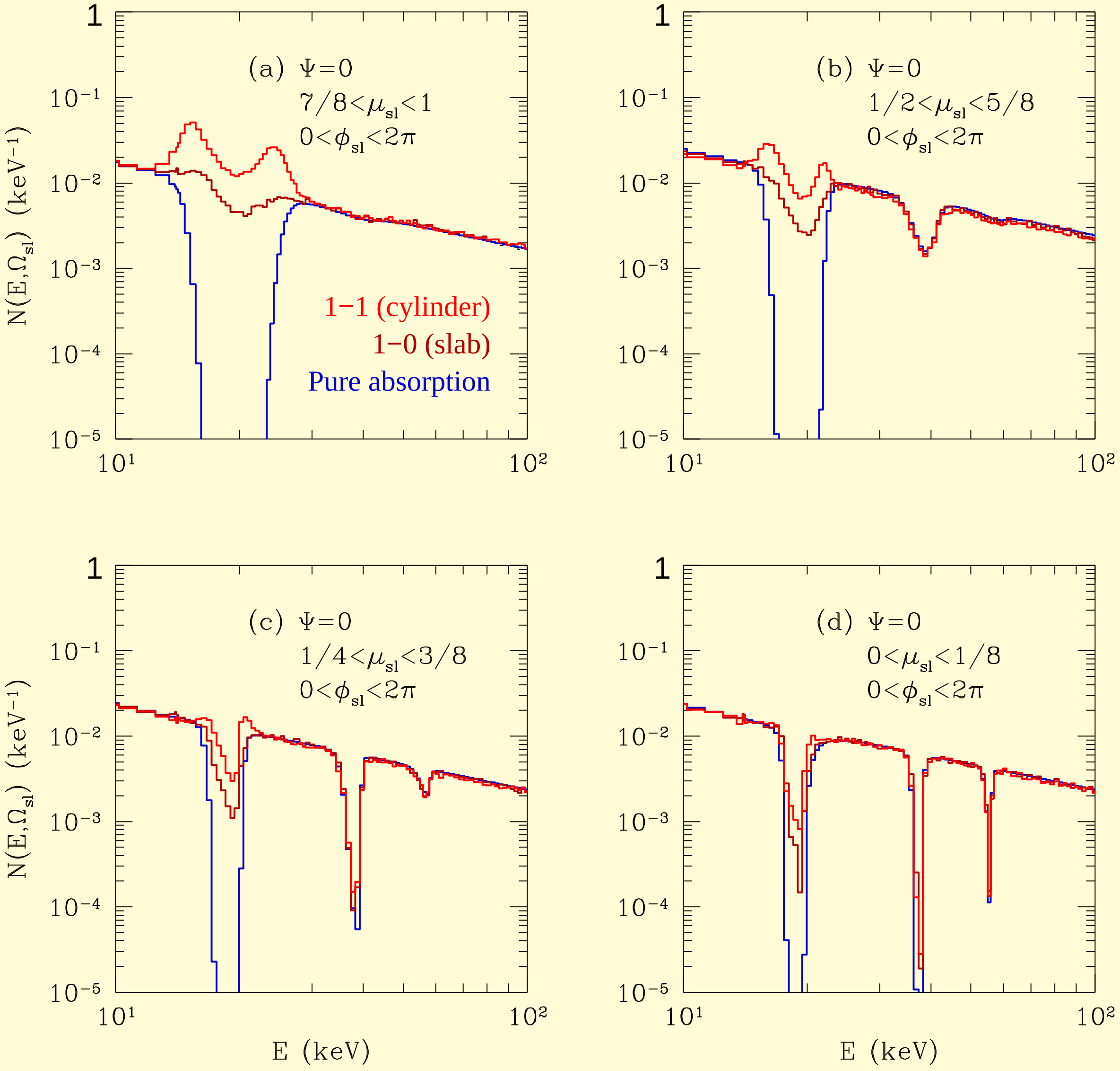

Isenberg, Lamb & Wang (1998b): dependence of the geometry on the CRSF shape

$\Longrightarrow$ see talks by Nishimura and Schönherr for more!

Continuum Formation: State of the Art

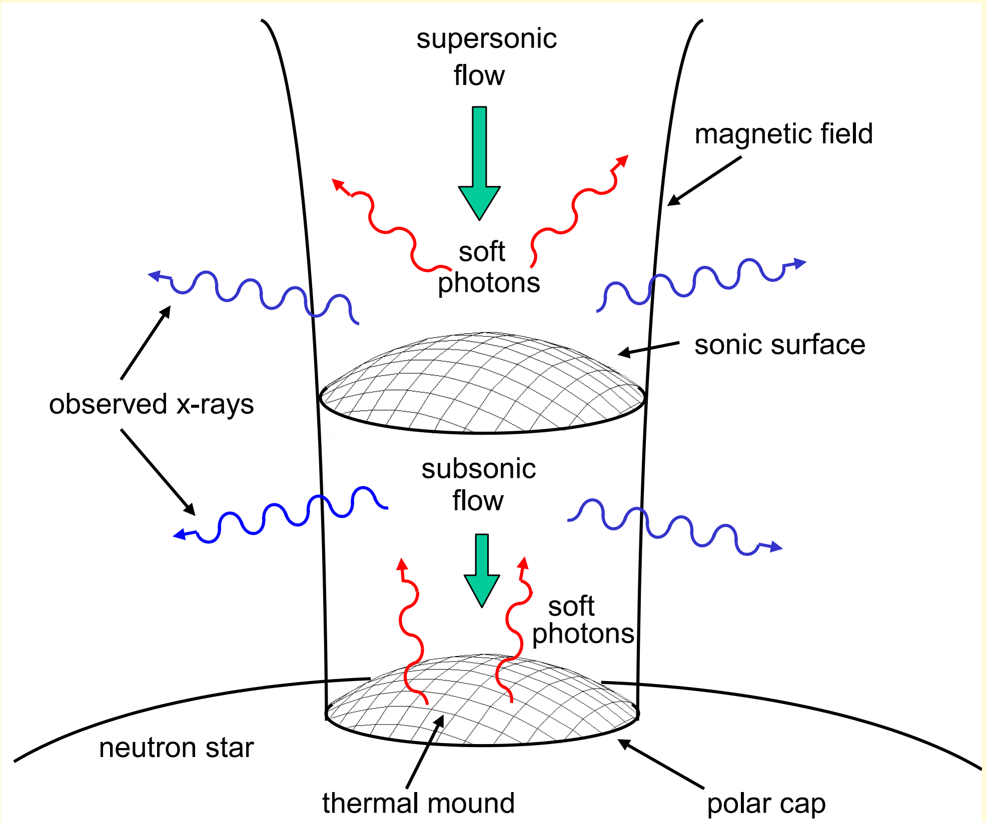

Becker & Wolff (2005a,b, 2007):

Previous work ignores accretion shock.

New picture: bulk motion Comptonization

- accretion mound produces soft X-rays
- X-rays are upscattered in accretion shock
- hard X-rays diffuse through walls of accretion column

$\Longrightarrow$ see next talks!

Conclusions

The major conclusions/questions of this contribution are:

1. Especially for wind accretion, structure of accretion flow only understood in a qualitative way

   $\Longrightarrow$ need to talk to accretion guys to try to get renewed interest in physics at the Alfvén radius!

2. Shape of accretion column: pencil vs. fan beam: not much work yet on how to constrain this observationally, on theory side stopping the flow still not understood for low L flows.

   $\Longrightarrow$ More needs to be done in this area!

3. CRSF line shape: importance of geometry, dependence on angle, etc.

   $\Longrightarrow$ Theory now good enough that comparison to observations possible.

   $\Longrightarrow$ Next talks

4. Column emission: much theoretical progress has been made in recent years

   $\Longrightarrow$ Next talks

Alexander, S. G., & Mészáros, P., 1989, ApJ, 344, L1

Araya, R. A., & Harding, A. K., 1999, ApJ, 517, 334

Arons, J., Klein, R. I., & Lea, S. M., 1987, ApJ, 312, 666

Basko, M. M., & Sunyaev, R. A., 1976, MNRAS, 175, 395

Becker, P. A., & Wolff, M. T., 2005a, ApJ, 621, L45

Becker, P. A., & Wolff, M. T., 2005b, ApJ, 630, 465

Becker, P. A., & Wolff, M. T., 2007, ApJ, 654, 435

Blandford, R. D., & Scharlemann, E. T., 1976, MNRAS, 174, 59

Blondin, J. M., 1994, ApJ, 435, 756

Braun, A., & Yahel, R. Z., 1984, A&A, 278, 349

Canuto, V., 1970, ApJ, 160, L153

Canuto, V., Lodenquai, J., & Ruderman, M., 1971, Phys. Rev. D, 3, 2303

Daugherty, J. K., & Harding, A. K., 1986, ApJ, 309, 362

Davidson, K., & Ostriker, J. P., 1973, ApJ, 179, 585

Freeman, P. E., Lamb, D. Q., Wang, J. C. L., Wasserman, I., Loreido, T. J., Fenimore, E. E., Murakami, T., & Yoshida, A., 1999, ApJ, 524, 772

Gnedin, Y. N., & Sunyaev, R. A., 1973, A&A, 25, 233

Gonthier, P. L., Harding, A. K., Baring, M. G., Costello, R. M., & Mercer, C. L., 2000, ApJ, 540, 907

Harding, A., & Lai, D., 2006, Rep. Prog. Phys., 69, 2631

Harding, A. K., 1994, in The Evolution of X-Ray Binaries, ed. S. S. Holt, C. S. Day, (Washington: AIP), 429

Harding, A. K., & Daugherty, J. K., 1991, ApJ, 374, 687

Harding, A. K., Mészáros, P., Kirk, J. G., & Galloway, D. J., 1984, ApJ, 278, 369

Heindl, W. A., Rothschild, R. E., Coburn, W., Staubert, R., Wilms, J., Kreykenbohm, I., & Kretschmar, P., 2004, in AIP Conf. Proc. 714: X-ray Timing 2003: Rossi and Beyond, ed. P. Kaaret, F. K. Lamb, J. H. Swank, 323

Inoue, H., 1975, PASJ, 27, 311

Isenberg, M., Lamb, D. Q., & Wang, J. C. L., 1998a, ApJ, 493, 154

Isenberg, M., Lamb, D. Q., & Wang, J. C. L., 1998b, ApJ, 505, 688

Karino, S., Kino, M., & Miller, J. C., 2008, Prog. Theor. Phys., 119, 739

Langer, S. H., & Rappaport, S., 1982, ApJ, 257, 733

Mészáros, P., 1984, Space Sci. Rev., 38, 325

Mészáros, P., 1992, High-energy radiation from magnetized neutron stars, (Chicago: Chicago Univ. Press)

Mészáros, P., & Nagel, W., 1985a, ApJ, 298, 147

Mészáros, P., & Nagel, W., 1985b, ApJ, 299, 138

Nagel, W., 1981a, ApJ, 251, 278

Nagel, W., 1981b, ApJ, 251, 288

Ostriker, J. P., & Davidson, K., 1973, in X- and Gamma-Ray Astronomy, ed. H. Bradt, R. Giacconi, 143

Pringle, J. E., & Rees, M. J., 1972, A&A, 21, 1

Schönherr, G., Wilms, J., Kretschmar, P., Kreykenbohm, I., Santangelo, A., Rothschild, R. E., Staubert, R., & Coburn, W., 2007, A&A, 472, 353

Ventura, J., 1979, Phys. Rev. D, 19, 1684

Wang, J. C. L., et al., 1989, Phys. Rev. Lett., 63, 1550